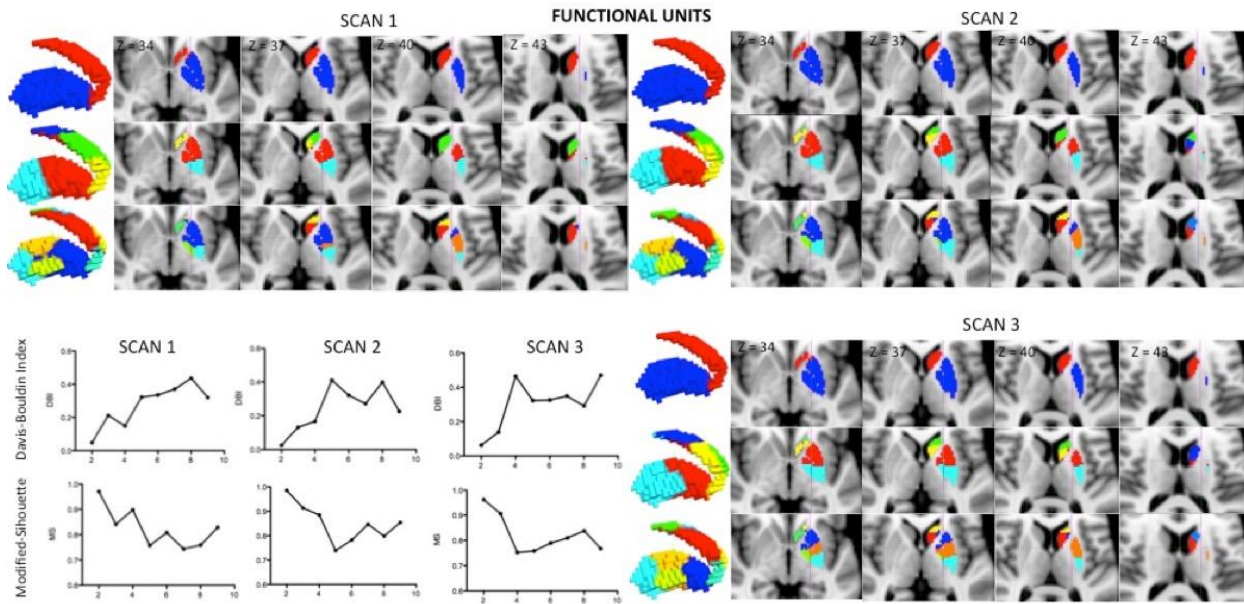
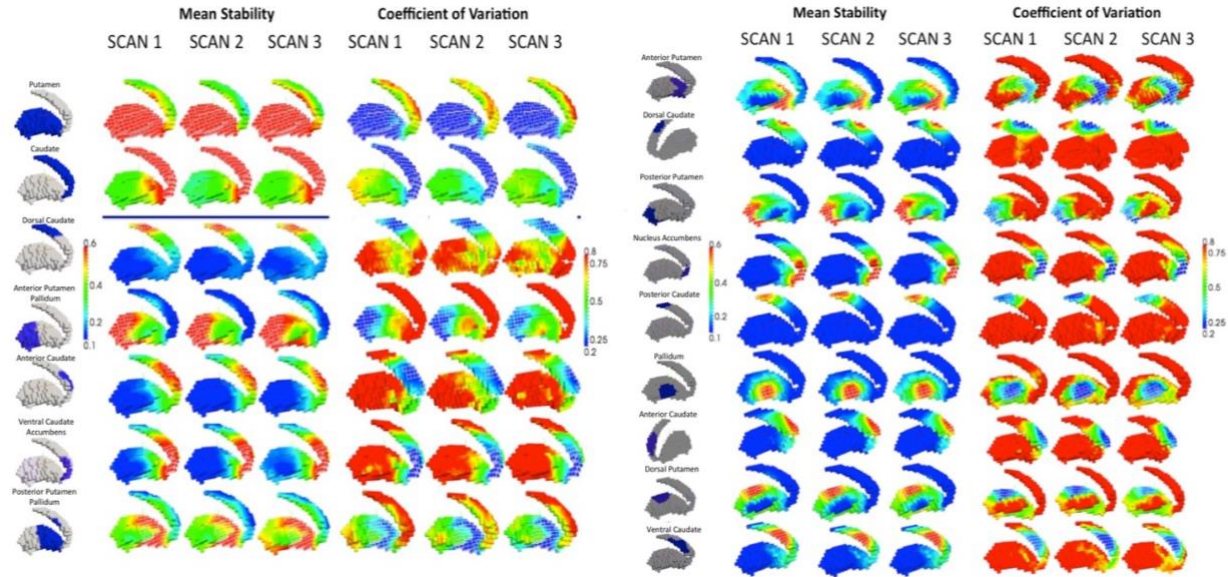


Supplementary Figures



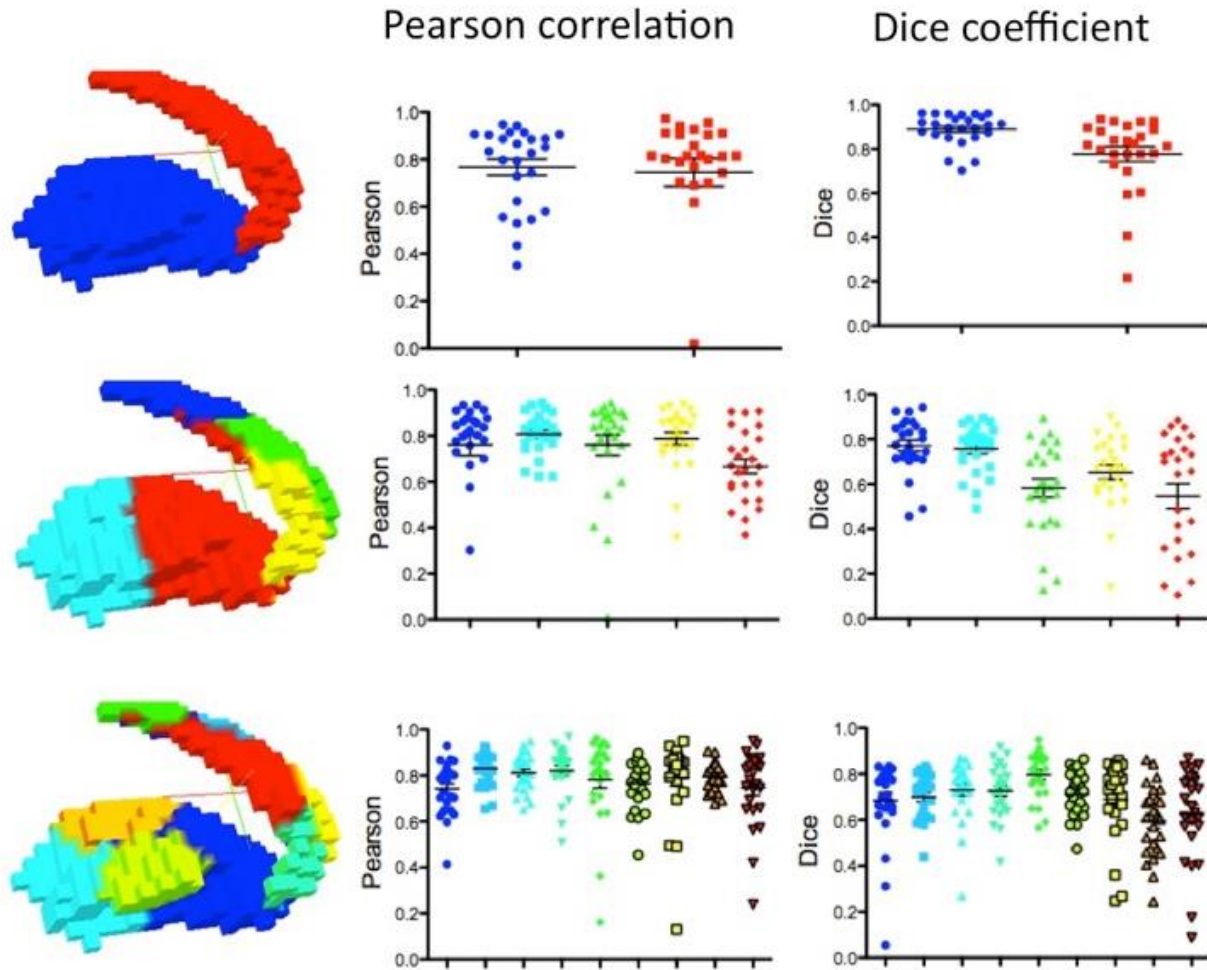
1128
 1129
 1130
 1131
 1132
 1133
 1134
 1135
 1136
 1137
 1138
 1139
 1140
 1141
 1142

Figure 1. Functional parcellation units for temporal resolution similarity measure. The group-level clustering of the BG in scans 1, 2 & 3 derive in very similar functional units. The 3D renders and sagittal views reveal a main partition of caudate and putamen at $k=2$, that remain in every resolution. While resolution $k=5$ divides the caudate into 2 units of ventral and dorsal/anterior areas, the putamen is sectioned into anterior and posterior units. The $k=9$ resolution shows a functional unit comprising nucleus accumbens and one for globus pallidum, while maintaining the tripartite caudate division of the $k=5$ resolution and dividing putamen into anterior, central and posterior units. Moreover, the Davis-Bouldin Index, a measure of within-cluster dissimilarity, and the Modified-Silhouette Index, a measure of between-clusters dissimilarity, point to 2, 4 and 9 as best performing solutions for scan 1; 2, 7 and 9 for scan 2; and 2, 5 and 8 as the best performing solutions for scan 3.



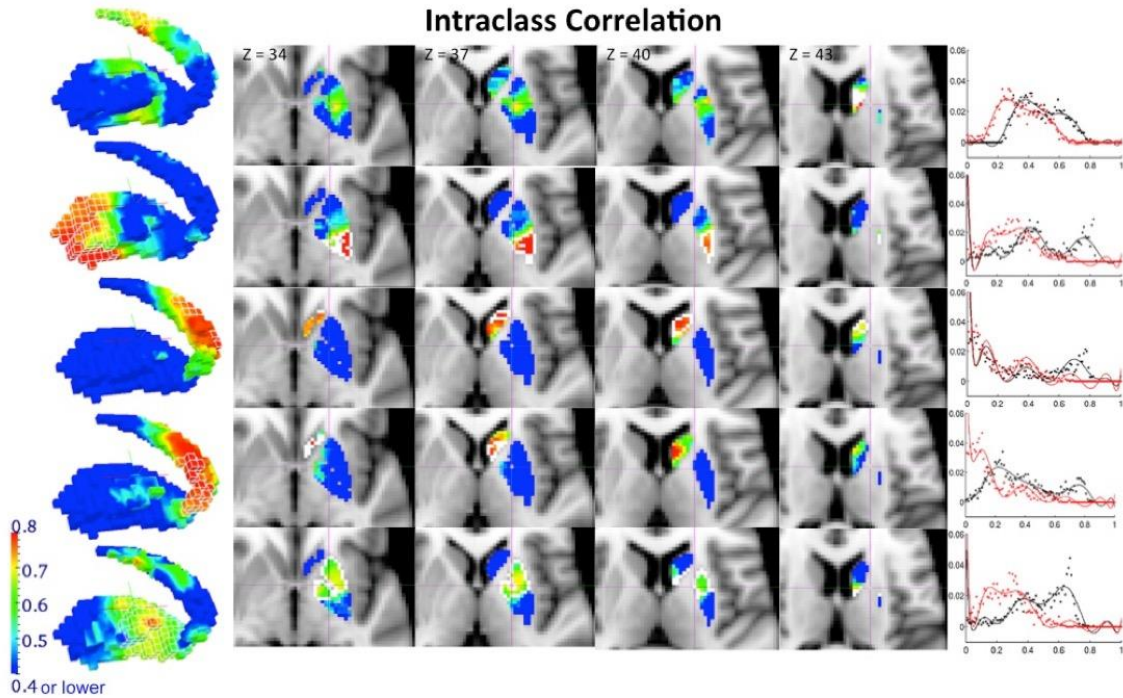
1143
 1144 **Figure 2.** (A) Mean stability and coefficients of variation for k=2 and k=5 resolutions on maps obtained
 1145 with temporal correlation as the similarity measure. The panels and renders show the average of the
 1146 stability maps across subjects for the 2 and 5 target clusters (shown on the first column renders and
 1147 delineated by a white wireframe on the 3D renders) of the k=2 and k=5 resolutions. All three scans show
 1148 very similar mean stabilities, with highest values within the target cluster and lower values distant from it.
 1149 The right columns show the coefficients of variation (standard deviation relative to mean) of the stability
 1150 maps across subjects for the 2 and 5 target clusters in the k=2 and k=5 resolutions. Again, all three scans
 1151 show very similar coefficients of variation, with lowest values within the target cluster and higher values
 1152 for voxels distant from it. (B) Mean stability and coefficients of variation for resolution k=9.

Reproducibility



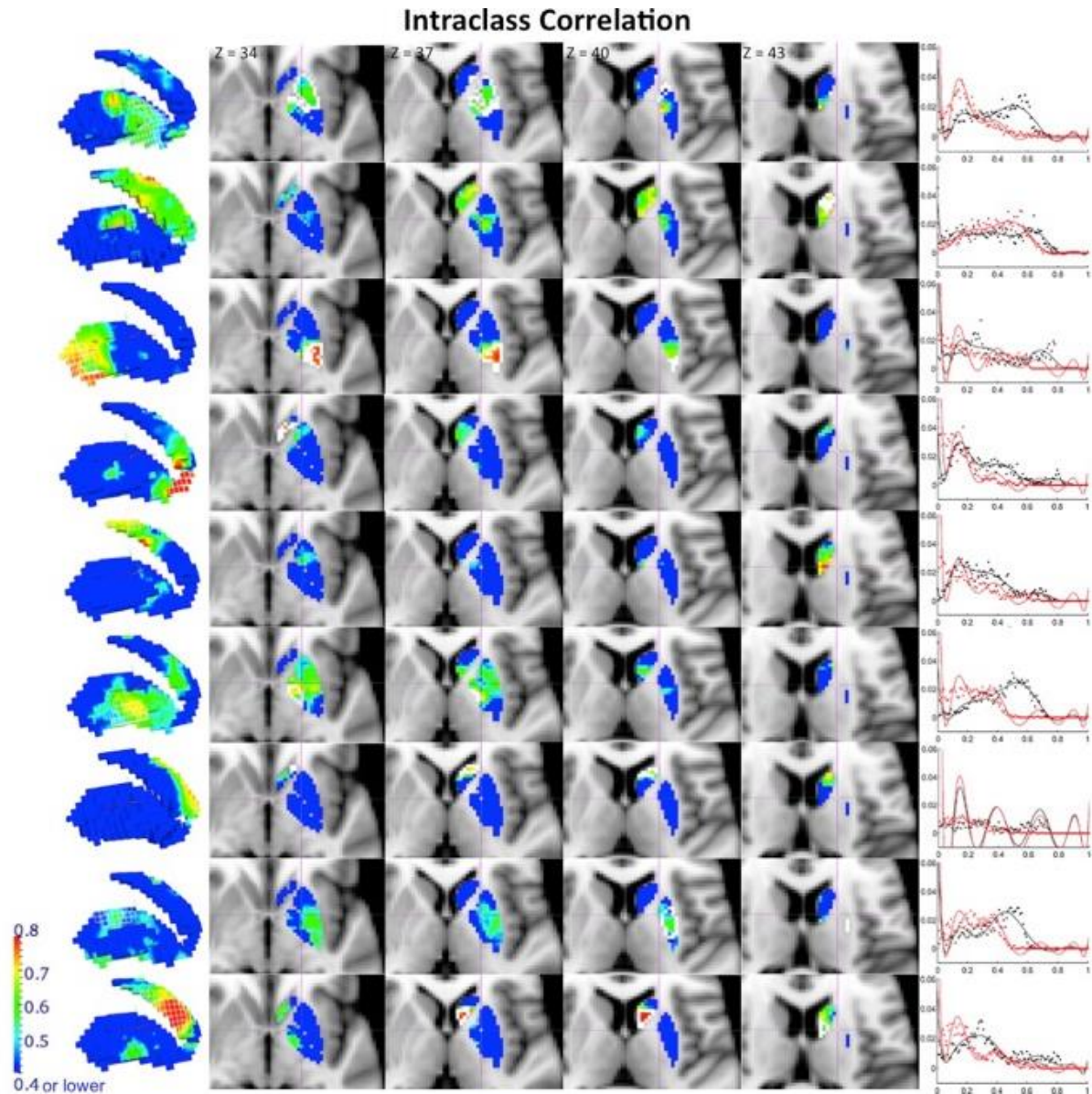
1153
1154
1155
1156
1157
1158
1159

Figure 3. Reproducibility of stability maps obtained by using the temporal correlation similarity measure. The 3D renders show the group-level functional units obtained for sessions 1 and 2. The plots indicate the reproducibility measured by Pearson correlation for each subject across stability maps obtained for resolutions $k=2$, $k=5$ and $k=9$. The Dice coefficient measured on binarized stability maps, in which 1 represents the most stable cluster, are also shown. These data reveal strong reproducibility of the stability maps obtained through BASC across different scans.

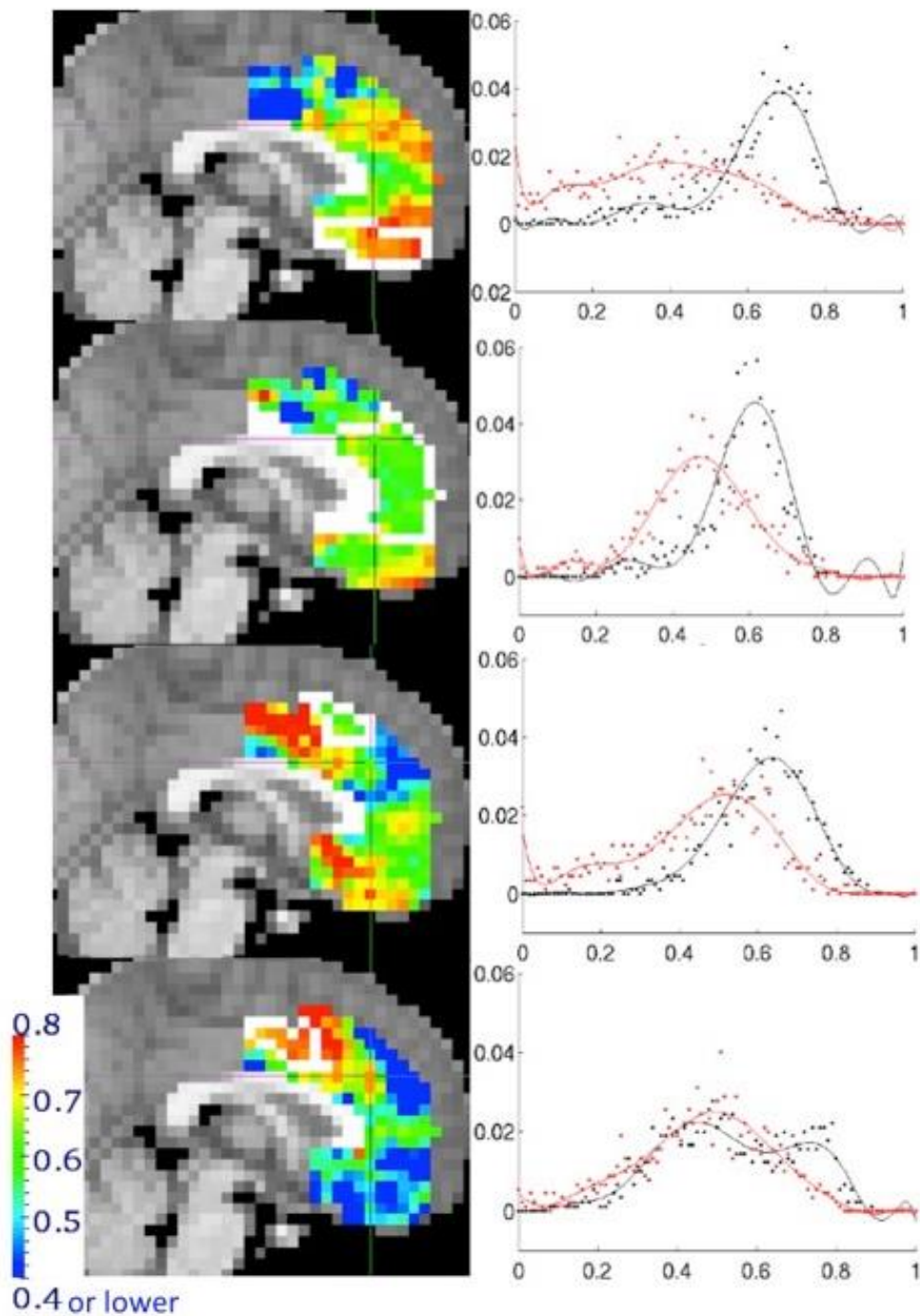


1160
 1161
 1162
 1163
 1164
 1165
 1166
 1167
 1168
 1169
 1170

Figure 4. Intra-class correlation (ICC) for maps obtained with temporal correlation as similarity measure with resolution $k=5$. We examined reliability at every voxel level through ICC in the stability maps, defined as the proportion of variability across subjects relative to the total variability in the data. ICC values for the stability maps obtained from scan 1 and the average of scans 2 and 3 at resolution $k=5$ are delineated by a white line for the slice view and a white wireframe on the renders. High ICC values are only found in proximity to the target clusters. The low stability in voxels distant from the target cluster might explain this regional distribution of ICC values in the BG. The graph placed next to each cluster's ICC map represents the distribution of frequencies of the ICC values obtained when ICC was computed after having regressed out mean frame displacement for each subject (in black), and also when ICC was calculated without regressing that parameter out (in red).

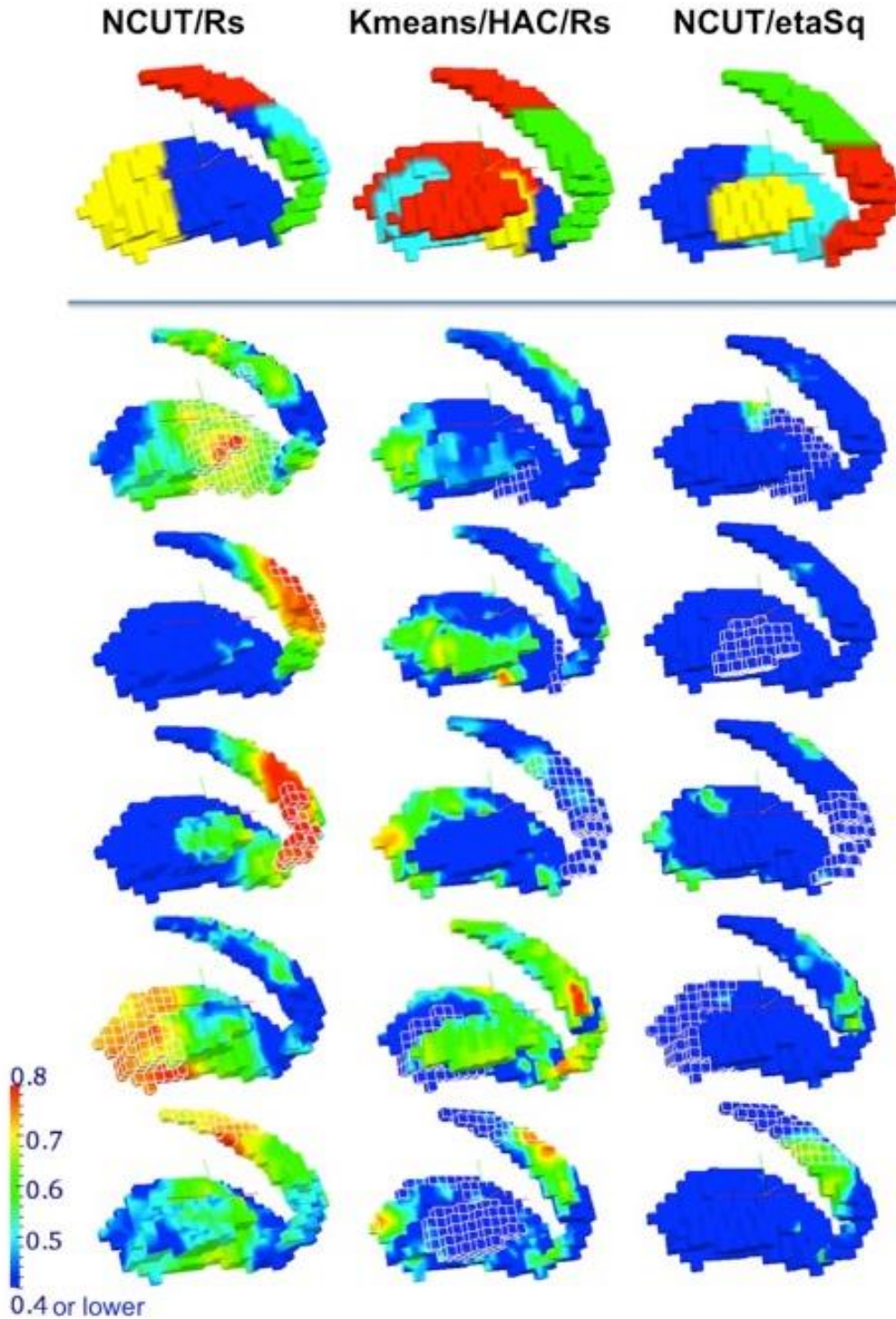


1171
 1172 **Figure 5.** Intra-class correlation (ICC) for maps obtained with temporal correlation as the similarity
 1173 measure with resolution $k=9$. We examined reliability at every voxel level through ICC in the stability
 1174 maps, defined as the proportion of variability across subjects relative to the total variability in the data.
 1175 ICC values between for the stability maps obtained from scan 1 and the average of scans 2 and 3 at
 1176 resolution $k=9$ are delineated by a white line for the slice view and a white wireframe on the renders.
 1177 High ICC values are only found in proximity to the target cluster. The low stability in voxels distant from
 1178 the target cluster might explain this regional distribution of ICC values in the BG. The graph placed next
 1179 to each cluster's ICC map represents the distribution of frequencies of the ICC values obtained when ICC
 1180 was computed after having regressed out mean frame displacement for each subject (in black), and also
 1181 when ICC was calculated without regressing that parameter out (in red).



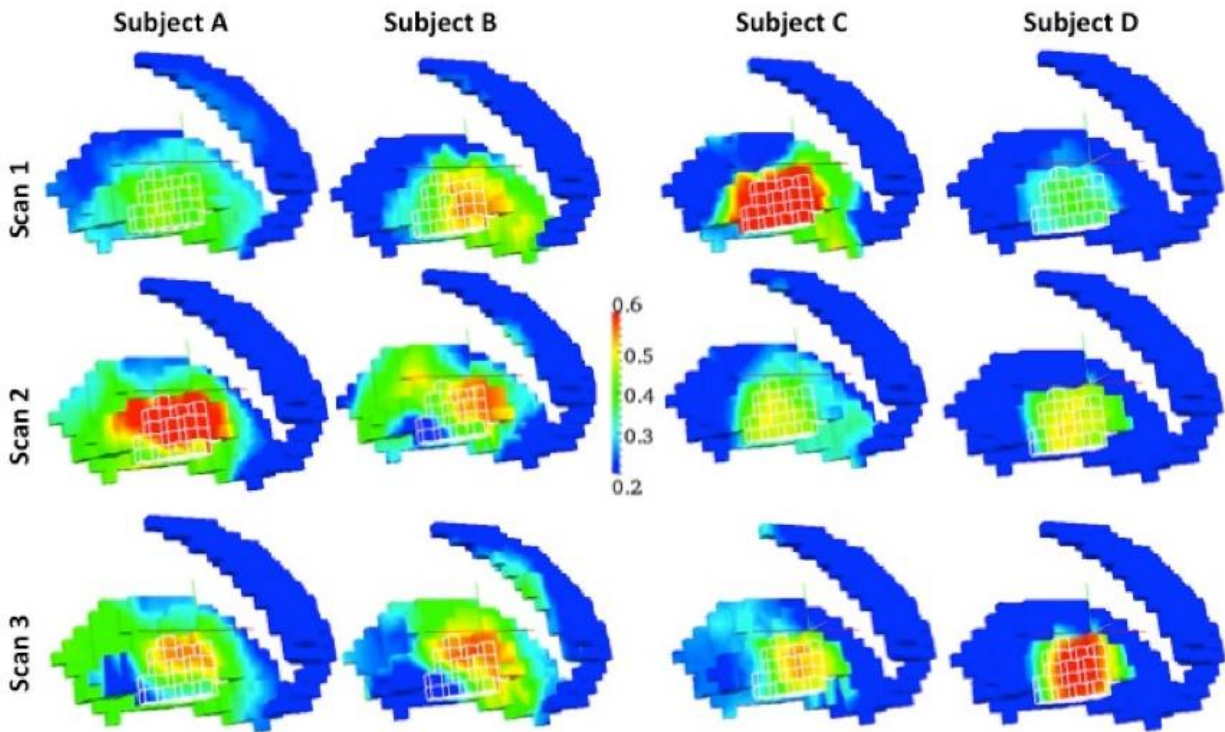
1182
 1183 **Figure 6.** Intra-class correlation (ICC) for maps obtained by applying BASC on a different brain region.
 1184 ICC values between sessions 1 and 2 in the TRT sample for the stability maps obtained from the medial
 1185 wall (target clusters delineated by a white line). Again, high ICC values are only found in proximity to the
 1186 target cluster. The low stability in voxels distant from the target cluster might explain the regional
 1187 distribution of ICC values in the BG. The graph placed next to each cluster's ICC map represents the
 1188 distribution of frequencies of the ICC values obtained when ICC was computed after having regressed out
 1189 mean frame displacement for each subject (in black), and also when ICC was calculated without
 1190 regressing that parameter out (in red).

1191



1192
 1193 **Figure 7.** Group-level divisions and ICC maps for stability maps obtained using (1) NCUT clustering and
 1194 spatial correlation as the similarity measure, (2) k-means clustering for the individual level analysis and
 1195 hierarchical clustering (HAC) for the group-level one, and spatial correlation as the similarity measure,
 1196 and finally (3) NCUT clustering and eta square as the similarity measure. K-means/HAC/Rs showed a
 1197 very unfeasible parcellation of the BG and lower ICC values with an unspecific distribution, while
 1198 NCUT/eta² displayed a feasible BG division, which differed from the one obtained by our method, with
 1199 low reliability.

1200



1201

1202

1203

1204

1205

1206

1207

1208

1209

1210

1211

1212

1213

1214

1215

1216

1217

1218

1219

Figure 8. Individual stability maps for four subjects across the three scans. Notice how for every subject and scan, the target unit, highlighted with a white wireframe, shows the highest stability values. It is interesting to notice that the most variability across subjects is found around the target unit's boundaries.